HHS Public Access

Author manuscript

Small Methods. Author manuscript; available in PMC 2021 July 21.

Published in final edited form as:

Small Methods. 2020 May 11; 4(5): . doi:10.1002/smtd.201900868.

Biological Interfaces, Modulation, and Sensing with Inorganic Nano-Bioelectronic Materials

Erik N. Schaumann, **Bozhi Tian**

Department of Chemistry, The University of Chicago, Chicago, IL 60637, USA

Abstract

The last several years have seen a large and increasing interest in scientific developments that combine methods and materials from nanotechnology with questions and applications in bioelectronics. This follows with a number of broader trends: the rapid increase in functionality for materials at the nanoscale; a growing recognition of the importance of electric fields in diverse physiological processes; and continuous improvements in technologies that are naturally complementary with bioelectronics, such as optogenetics. Here, a progress report is provided on several of the most exciting recent developments in this field. The three critical functions of biointerface formation, biological modulation, and biological sensing using newly developed nanoscale materials are considered.

Keywords

bioelectronics; bioelectronic sensors; modulation; nanostructures; semiconductors

1. Introduction

The study of electromagnetism in the biological setting has been of interest to researchers since the earliest physical descriptions of electricity.[1,2] Developments in electrical devices have frequently been accompanied by discoveries in electrophysiology, perhaps most notably in the period 1949–1952, when the application of microelectrodes[3] and differential amplifiers[4] (and later operational amplifiers) facilitated the voltage clamp methods employed by Hodgkin and Huxley to posit a mathematical description of action potential propagation in squid giant axons.[5,6] As electronic devices have scaled down into the microscopic and nanoscopic regimes, we find ourselves faced with a large and widening frontier of interesting questions in the field of bioelectronics, the interface of research in biology and electronics.

Electronic devices with micron- or even sub-micron-scale features have been the unifying feature of a number of very exciting bioelectronics applications in the last several years. Utah and Michigan-style microelectrode arrays for neural sensing are undergoing continuous

btian@uchicago.edu.

The ORCID identification number(s) for the author(s) of this article can be found under https://doi.org/10.1002/smtd.201900868.

Conflict of Interest

The authors declare no conflict of interest.

miniaturization efforts,[7,8] allowing for improved resolution and less invasiveness.[9] Closed-loop systems, in which sensing, modulation, power, and control are all present in a self-contained unit, represent a frontier in this line of research.[10] Applications that integrate these devices in larger systems have already yielded impressive results, such as a bionic hand with sensory feedback,[11] and a closed-loop optogenetic system that can modulate bladder function in rats.[12] These developments provide us with a helpful template for the future of nano-bioelectronics. In the coming years, we expect to see a proliferation of integrated devices and closed-loop systems that incorporate nanoelectronics in biological contexts.

Nanoelectronics present us with a number of features that make them particularly desirable in biological research. Nanomaterials can possess unique optical,[13] electronic,[14,15] and magnetic[16,17] properties that only become evident at sufficiently small length scales. Moreover, nanoelectronics provide the opportunity to probe the coupling of electric phenomena and physiology from the scale of tissues and organs down to the scale of individual cells and organelles (Figure 1).[18–21] The ability of these materials to target such small structures opens the door to inquiries into the pathways for electrical transduction in biology at the scale of the pertinent molecules, and to leverage those to access therapeutic targets that would otherwise be unavailable.

We draw a contrast here between inorganic nano-bioelectronics, which are the focus of this Progress Report, and organic nano-bioelectronics, which are also a subject of intense research. Inorganic devices in this context are typically made from semiconductor or metal materials, while organic ones are primarily carbon-based and may be derived from biological sources. Organic devices have shown great promise as bioelectronics, and we refer the reader to a small selection of the numerous excellent articles regarding nanodiamonds,[22–26] carbon nanotubes,[27–29] and graphene-based materials[15,30,31] as well as conjugated polymers[32] and biologically-derived nanomaterials.[33,34]

In broad terms, the advantages of inorganic nanomaterials are that they can adopt a wide array of precisely tunable architectures and functionalities, which can be achieved through numerous techniques during synthesis.[15,35–38] Their disadvantages include potentially high costs of manufacture, particularly with respect to noble metal precursors,[36,39] and the possibility for accumulation without degradation in cells.[40,41] Organic nanomaterials tend to have good biocompatibility when functionalized appropriately.[23,26,32,42] They also integrate well with other bioelectronic tools, either as extensions to scaffolds[32] or as the scaffolds themselves,[33] and they can minimize negative cellular responses to mechanical mismatches between the cytoskeleton and the device.[32,33] Compared to inorganic devices, however, the number of available form factors is comparatively few, and the degradation of some materials may limit applications for long-term experiments and treatments[32,43]

The three critical functions of nano-bioelectronics that we have selected as our focus of attention are biointerface formation, modulation, and sensing. All three of these aspects have seen a number of exciting developments using inorganic devices in the last few years. Because any putative functionality depends on interface formation, a number of recent reports include advancements in forming new types of interfaces that in turn enable access to

new modes of modulation or sensing. Where necessary, we have divided the pertinent parts of each publication into the corresponding sections. We hope this will aid the reader in rapidly locating relevant information.

2. Interfaces

One of the first questions any bioelectronic device must address, irrespective of the scale or nature of the device, is that of the interface. The nature of the device–target interface is frequently the most important factor in determining the modes of access to modulation or sensing. As such, there exists considerable interest in developing and characterizing new types of interfaces, for the purposes of extending the functionality of these devices, as well as understanding side effects that may accompany integration.

2.1. Intracellular Interfaces

Intracellular devices for bioelectronics are less common than extracellular interfaces, as one might expect on the basis of the additional challenges of getting them inside of cells. Despite the added complexity of identifying internalization mechanisms, intracellular interfaces possess many desirable properties. Because they pass the plasma membrane, intracellular devices can target particular organelles,[21] which extends the range and specificity of functionality. This allows for techniques that mimic the high spatial and temporal resolution of optogenetic methods,[44] without requiring any genetic modification. They also are typically less invasive then devices that rely on extracellular interfaces.[40,41,45] Completely intracellular methods would hypothetically require only a syringe injection to a target location,[46,47] with no additional surgery or attachment procedures required—similar to the conventional delivery of drugs. Moreover, they are requisitely free of external connections, such as wires that extend outside of the organism.

A direct technique for crossing the plasma membrane is microinjection, in which materials such as tracking particles[48] or DNA[49] are delivered to the intracellular space through a micropipette. The last few years have seen the development of nanoscale devices that are less invasive than microinjection, while offering a similar capability for payload delivery. Arrays of substrate-bound silicon nanoneedles have been fabricated to develop a nanoinjection platform that is capable of delivering genetic constructs,[45] quantum dots,[41] and endocytic pathway-specific payloads[50] to cells and tissues, with little negative biological impact over the course of 60 h (Figure 2A).[45] Likewise, arrays of nanostraws, that is, inorganic hollow nanotubes that permit fluid flow within the cavity, have been used for both delivery to and sampling from the intracellular space. Specifically, they can deliver membrane-impermeable secondary messenger molecules[51] and markers of protein glycosylation[52] to cells (Figure 2B), as well as to repeatedly acquire samples of intracellular fluid for analysis over a period of up to five days.[53]

Intracellular delivery of freestanding devices is typically based on accessing cells and tissues by leveraging some endogenous means of internalization. Certain devices require little or no modification to enter cells. Silicon nanowires (SiNWs), for instance, are spontaneously internalized by several cell types (Figure 2C)[40] and can be used for several modalities of stimulation, which will be discussed further in Section 4. Cell types that do not internalize

SiNWs can still be accessed, if they are in close communication with other cell types that do. Cardiomyocytes (CMs), for instance, do not form interfaces with nanowires (NWs) but under some circumstances they form contacts with cardiac fibroblasts, which do. Therefore, to engineer a noninvasive application of NWs with CMs, fibroblasts with internalized NWs can be added to in vivo hearts and allowed to integrate with the native tissue (Figure 2D).[54]

Other devices may be internalized through the use of specific components on the surface, which are recognized by the target cells. Rod-shaped core/shell CdSe/CdS nanoparticles can be differentially localized to neuron plasma membranes by varying the surface charge, for example.[55] A variety of conjugation techniques have also been employed for neural targeting of quantum dots.[56–58] In each of these cases, recognized peptides were used to facilitate quantum dot entry into the cells. A similar approach was taken in recent work using upconversion nanoparticles (UCNPs), wherein the UCNPs were functionalized with concanavalin A protein, such that they bound to individual photoreceptors to form hybrid systems termed nanoantennae.[46]

2.2. Extracellular Interfaces in Planar Configurations

An extensive body of work exists on devices that form extracellular interfaces. This includes interfaces on the scale of individual cells and colonies in 2D culture,[59,60] collections of cells cultured in 3D,[61,62] over the surfaces of organs,[63] as well as both in vitro[63] and in vivo[54] contexts.

One approach for forming interfaces entails simply adhering cells on the surface of materials with the desired characteristics for sensing or stimulation. Relevant considerations here include the ability for cells to adhere on a given surface as well as the nanoscale topography of the surface.[64,65] A third important facet is the mechanical match between material and tissue.[66] While certain characteristics of cells, such as the mechanical work they perform per unit area,[67] are invariant under changes in substrate stiffness within physiological ranges, significant impacts can manifest, ranging from changes in cell spread area[66] to the fate of differentiation in stem cells.[68] Most solid substrates are considerably stiffer than biological environments, with, for example, the Young's Modulus of glass at ≈50 GPa,[69] compared to the kPa values seen in biomimetic substrates.[67] In order to attenuate the impact of stiffness mismatches, then, extracellular interfaces must therefore be inherently soft, or else embed stiff materials in softer carriers.

Heterogeneous porous silicon substrates can be composed from hexagonal lattices of SiNWs crosslinked by Si "micro-bridges."[59] These constitute a class of materials that retain some semiconductor characteristics, but become more mechanically compliant in phosphate-buffered saline solution. Interestingly, they also bear a passing similarity to the microscale structure of bones.[59,70] While the stiffness of these structures, in the range of MPa, is still considerably higher than that of most in vivo tissues, both their mechanical characteristics and their microstructure suggest them as useful scaffolds for mimicking bone tissue. Doped silicon can also be deposited onto silicon-on-insulator (SOI) wafers to form planar substrates,[60] or Si membranes. The doping profile can be controlled during deposition, so that different optical responses can be achieved. Cells are still adherent on the surface of these membranes, however, the device itself is both materially and structurally closest to

bulk silicon. As a result, cells grown on the surface of Si membranes adopt the morphology of cells grown on non-biomimetic substrates, such as glass.

2.3. Extracellular Interfaces in Three Dimensions

Cells natively grow in a soft 3D environment, rather than the hard 2D surfaces that typify many cell-scale experiments. This difference in environment is known to alter morphology on the individual cell and tissue scale,[71] as well as electrophysiology.[72] This provides a natural motivation for designing devices that can interface with tissues and organs in 3D. In order to form tight interfaces, these devices can provide a predefined biomimetic scaffold for tissues.[62,73] An alternative approach is to work with devices that are flexible at the relevant length scale. This has been accomplished recently with microelectrode arrays (MEAs)[61] on the scale of organoids, as well as on the tissue scale by embedding p-i-n SiNWs in a polymer mesh and placing the entire structure around ex vivo rat hearts.[63] In all cases, the same mechanical considerations that apply in 2D are also valid in 3D: any potential candidate device should comprise features on the cellular length scale[73] and have similar compliance to that of extracellular matrix.[61]

Nanoelectronic scaffolds were first synthesized as dispersed silicon nanowire field effect transistors (SiNW-FETs) in a network of ribbons of polymer and metal interconnects (Figure 3A).[73] During synthesis, the configuration of the polymer ribbons and metal interconnects could be specified by electron beam lithography and selective metal deposition. Because this process took place on a nickel relief layer, the metal interconnects could be designed to have desirable mechanical characteristics after the device was lifted off. Specifically, if the metal was deposited symmetrically as a lattice, the interconnects would remain unstressed after lifting off, and the resulting scaffold would remain as a 2D mesh. The final 3D structure could then be defined by folding or rolling. Conversely, nonregular or otherwise asymmetric metal deposition yielded metal interconnects in a stressed configuration. When these devices were lifted off, the extant stresses compelled the scaffold to adopt a 3D conformation. In both cases, the result was a freestanding 3D structure with integrated nanowires, which was moreover flexible and macroporous. These devices could then be integrated with ECM or other macroporous biomimetic materials, yielding a substrate that was competent for cell culture in 3D as well as sensing from each field effect transistor (FET).

The principle of engineering residual stresses in a 2D structure to form a final 3D structure has been applied more recently to fabricate a microelectrode array for electrical sensing of cardiac spheroids.[62] In that work, graphene FETs were patterned on SU-8 using conventional lithography and interconnected with metallic electrode lines composed of successive layers of chromium and palladium. The metal layers could be produced with tensile residual stresses, such that the device had a propensity to roll itself up, and the final radius of curvature was tunable by varying the SU-8 thickness. The resulting tube structure (Figure 3B) could be unrolled and a CM spheroid transferred to the surface, so that upon release the majority of the surface of the spheroid was covered by the device. The spheroids integrated with the sensor array without apparent damage to the component cells, allowing for multiplexed electrophysiological recording from the array. The radius of curvature was

controllable, meaning that future interfaces could be formed with spheroids and organoids of different sizes.

The last several years have seen the development of nanoelectronic devices with exceptional mechanical compliance.[47,61] Such devices offer functionalities that are inaccessible to traditional electronics, in addition to the enhanced biocompatibility that comes with devices that more closely match the extracellular environment of tissues. An especially dramatic example of this principle is in the development of syringe-injectable electronics,[47] first reported in 2015. These devices are similar to the nanoelectronic scaffolds in that they were composed of a mesh structure containing both polymer and polymer/metal interconnects. As designed, the mesh is very stiff in the direction of injection, so as to preclude buckling of the structure, but very compliant in the transverse direction. This allows the overall structure to be compacted down enough to fit through needles with a diameter as small as hundreds of μm (Figure 3C). After the compacted mesh passes through the needle, it can then expand back out and interface with in vivo structures. An example case of this has been shown in injecting a mesh into rodent brains, where the mesh was successfully integrated with the brain structure and was used to record electrical activity.[47]

Other recent work has focused on producing nanoelectronic devices that are flexible enough to conform to the 3D structure of their target, rather than providing a predefined structure.[47,61,74] A notable recent demonstration of this was presented by Li and coworkers,[61] in which a mesh MEA interfaced with cocultures of human mesenchymal stem cells and human induced pluripotent stem cells in two dimensions, and adjusted to match the conformation of the tissue as it folded to form a 3D, spherical organoid (Figure 3D). The essential component to this ability came from the design of the mesh, where the interconnects between electrodes followed a serpentine pattern. This allowed for the overall mesh to undergo both stretch and compression deformations while retaining its structural integrity. Additionally, the small dimensions of the device components resulted in low bending stiffness, such that the forces generated during organogenesis well exceeded the threshold required to enact the required shape changes in the mesh. As a result, the device remained interfaced with the organoid throughout organogenesis, and could record electrical signals for the duration of the process.

Another approach to flexible bioelectronic interfaces is to incorporate freestanding devices with polymer substrates, thus retaining the electric functionality as well as the mechanical characteristics of the polymer. This method is broadly compatible with biological systems to the same extent as the supporting matrix. PDMS substrates have been used in conjunction with planar Si diode junctions to yield flexible devices that conform to the surface of brains.[60] Similarly, silicon nanowires embedded in SU-8 matrix have been observed to interface with ex vivo hearts.[63]

3. Modulation

We are amidst a period of growth for bioelectronics—given the toolkit afforded to us from molecular biology, we can now seek to ascertain the roles of each component in response to electrical stimuli. A substantial amount of bioelectronic work has been conducted using

macroscopic devices,[75–77] but new developments allow us to modulate bioelectronic responses with high spatial resolution, from the scale of tens of nanometers[60,78] to the size of organs.[60,63] In this way it is similar to the advancements being made using optogenetic techniques that have high spatiotemporal resolution relative to systemic genetic manipulations.

We can split modulatory devices into two broad categories, based on whether or not they are freestanding (leadless). In a therapeutic context, freestanding devices offer the advantage of being significantly less invasive to deliver, and their inherently smaller scale means they can be more precisely targeted to specific structures.[40] Substrate-bound or wired devices, on the other hand, can be easily connected to devices that allow for the precise control over the strength and timing of stimulating pulses, as well as recording capabilities.[79]

3.1. Mechanisms of Optical Response in Freestanding Devices

Among freestanding devices, optically responsive materials are especially appealing because of their fast response time, the ubiquity of light sources that are usable for stimulation, the wide variety of available form factors, and the ability to tune the contributions of different photoresponses. The nature of these responses can be to generate heat (photothermal),[60,80] generate a capacitive current (photocapacitive),[60] induce redox reactions (photofaradaic),[44] or to re-emit photons, which can proceed through fluorescence[22] or upconversion[81] mechanisms.

Semiconductor nanomaterials, like their macroscopic counterparts, are particularly useful for photocapacitive and photofaradaic applications.[82] Both cases rely on the same fundamental process, wherein photons generate electron–hole pairs in the depletion zone of p-i-n junctions, and the resultant charge separation compels some sort of electrical response.[83] Because biological media are rich in electrolytes, the unstimulated state of these materials is defined by the presence of an electrical double layer around the surface. The photo-induced perturbation first disrupts the double layer in what is termed the capacitive response, a large and rapid change in the electrical potential (Figure 4A). Continued optical stimulation further results in an increased concentration of charge carriers on the device surface, depending on whether the outer material is n-type (electrons) or p-type (holes). The presence of these carriers can induce redox reactions for the duration of the optical stimulation—the photofaradaic response (Figure 4A-C). Finally, amid any photoresponse there is the possibility of electron-hole pairs undergoing nonradiative recombination, which produces phonons that ultimately drive the photothermal response.[83] Defect-laden structures can display an enhanced photothermal response, owing to defect-induced conical intersections within the range of the band gap that facilitate nonradiative recombination.[84]

In a biological setting, the photocapacitive, photofaradaic, and photothermal responses may all be able to alter the membrane potential of cells. Because the first two processes directly relate to the manipulation of local electric fields, it is reasonable to expect that they can actuate voltage-gated channels that are responsible for regulating the overall cell membrane potential.[85,86] In the case of photothermal modulation, the change in potential is postulated to arise from the temperature-dependent electrostatic characteristics of cell membranes.[87,88] In particular, the double-layer capacitance increases with increasing temperature,

[59,88] while the impedivity decreases,[87] such that the localized heating yields a depolarizing current, that is, an inward flux of positive ions. In the following discussion, we will direct our particular focus to the calcium ion, Ca^{2+}, as a particularly notable signaling pathway that can be activated as a result of such depolarizations.

3.2. Calcium as a Target for Device-Driven Modulation

Calcium signaling presents one appealing target for modulation by means of nanoscale devices, as it possesses a singular importance in cell physiology and can be regulated in part by electric fields. Calcium ion, Ca^{2+}, is a classic secondary messenger molecule, and in this context is implicated in processes as diverse as wound healing,[89] cardiac pacing,[90–91] and pathogen recognition in plant cells.[92] The best representative of the functionality of Ca^{2+} is calmodulin (CaM), a protein that has persisted largely conserved for ≈1.5 billion years.[93] CaM changes its conformation in response to Ca^{2+} binding (Figure 5A), enabling it to be recognized by CaM binding sites found on a large number of proteins, and as such acts to translate changes in Ca^{2+} concentration to protein regulation.[93] Its expression is responsible for laying the foundation of different beak morphologies in Darwin's finches.[94,95] On the scale of cells and tissues, it is also involved in diverse physiological processes, such as maintaining smooth muscle tone[96] and cytoskeletal regulation.[97]

Photocapacitive and photofaradaic materials are strong candidates for applications in localized Ca^{2+} stimulation. Silicon p-i-n diode junctions and coaxial p-i-n silicon nanowires (SiNWs) have both been used to induce Ca^{2+} fluxes in response to illumination in dorsal root ganglia (DRG).[44,60] The simplest, presumed mechanism for this Ca^{2+} response is that it is actuated directly, by a change in local membrane potential that operates voltage-gated calcium channels.[93] That being stated, there are certainly other possible means by which electrical stimulation can have physiological effects, in calcium-dependent and independent ways.[75,76,98] These tend to be most applicable for long term exposures on the scale of tissues,[75,76] which renders the putative benefits of optical stimulation with nanoscale devices irrelevant when coupled to these mechanisms. As such, we will focus our attention on Ca^{2+} stimulation and directly related processes in the context of standalone devices.

3.3. Silicon Nanowire Interfaces for Optical Modulation

SiNWs are capable of eliciting Ca^{2+} responses through a primary photofaradaic stimulation,[44] but other related materials may also act through photocapacitive[60] and photothermal[99] mechanisms. They have a low but noticeable capacitive response, a strong faradaic response, and a low but nonzero photothermal response.[60] The photothermal response can be tuned by adjusting the porosity of the NWs by way of metal-assisted chemical etching.[99]

A few recent works have used p-i-n SiNWs with the specific aim of modulating Ca^{2+} signaling in cardiomyocytes (CMs), which is, functionally, equivalent to modulating the pace of beating in those cells.[54,63] Because CMs do not readily internalize whole NWs, the approaches presented in each work differ based on their method for forming NW-CM interfaces.

The first method sought to program CMs to adopt a target beating frequency through repeated training sessions, performed on a polymer mesh-SiNW substrate. The SU-8 mesh-

based approach relies on the interfaces formed between cells and NWs embedded in the polymer substrate.[63] While the device is macroscopic, the stimulation relies only upon the photofaradaic response of the NWs, so the overall technique remains leadless. By using a scanning confocal microscope for illumination, stimulation times and locations may be precisely defined by taking into account the scan rate of the system, the size of the relevant airy disk, and the position of the stimulated NWs. The authors defined training periods subject to stimulation at the desired beating frequency as well as rest periods, and monitored the fluorescence of a Ca^{2+}-sensitive dye to find the post-stimulation beating rate. CMs cultured on the mesh substrate could be trained to beat in a target range between 500 and 1200 mHz within four training periods. Furthermore, the flexible mesh could be applied around whole ex vivo hearts, which spontaneously formed interfaces without the need for additional surgical procedures. The target beating rates were set to 1 and 2 Hz, and each rate could be achieved within 400 s of stimulation. This demonstrated the effectiveness of mesh-based photofaradaic devices for cardiac pacing in cell culture as well as entire hearts.

An alternate, recently presented, method for accessing CMs with SiNWs involved taking advantage of supporting cell types that spontaneously internalize the NWs, and relying on coupling between those cells and CMs.[54] For putative therapeutic applications, this technique presents the benefit of being minimally invasive, as it requires only an injection of NW-containing cells, provided the given cells interface with the CMs. In the report, myofibroblasts (MFs) were selected as candidates because they fulfill the criterion of internalization, and because they are the subject of a debate regarding their competency for electrical coupling with CMs.[100,101] Optical stimulation of NWs in cultures of MFs produced clear Ca^{2+} responses in the cells, which appeared to then transmit the Ca^{2+} signal intracellularly (Figure 5B). Moreover, in co-cultures of CMs and MFs, stimulation in MFs was recognized by adjacent CMs very rapidly, and much like stimulation using the mesh-based devices, CMs could be trained over the course of about 400 s to beat at a desired frequency. Interestingly, this same level of communication was not evident in whole hearts, where Ca^{2+} responses were typically limited to the specific cells being stimulated.

Within the in vitro context, Parameswaran and co-authors have used coaxial p-i-n SiNWs to elicit action potentials in cultured neurons (Figures 4C,5C,D).[44] In the system studied, gold nanoparticles were used as a catalyst in the chemical vapor deposition-based synthesis, and remain on the final product as metallic gold centers along the NW surface. These gold centers were posited to alter the surface states of the silicon, which facilitated a photofaradaic response to optical stimulation at 532 nm. Cathodic reactions dominated this response, since the shell was composed of n-type silicon, whereas the exposed surface of p-type silicon was comparatively lower. When these NWs were added to a culture of dorsal root ganglion cells, they interfaced with the cells, and the photofaradaic reaction could induce action potentials using laser power as low as 6.75 mW for 1 ms (Figure 5C,D). This included single action potentials, as well as trains at up to 20 Hz.

An alternate type of device can be formed from SiNWs crosslinked by Si nanobridges, which yields a material that is chemically heterogeneous and mesoporous (see Interfaces).[59] Electrical modulation from these devices is achieved indirectly, through the photothermal effect, rather than through photocapacitive or photofaradaic means. The

induced local heating around membranes reduces impedance across the membrane and facilitates a depolarizing current. Micron-scale segments of this material have been added to DRG cultures, where they form extracellular interfaces with the component cells. Photothermal stimulation of these interfaces yields the expected depolarization, which triggers action potentials. As such, these materials offer another method for neural modulation, which does not rely on internalizing the relevant structures, as is required with nanowires, but can also be deployed on a subcellular scale.

3.4. Planar Silicon Substrates for Optical Modulation

Silicon devices with geometries distinct from nanowires can exhibit markedly different responses.[60] Planar p-i-n diode junctions have similar dopant profiles as coaxial SiNWs, but the layers form thin membranes on the wafer surface, rather than adopting a core-shell morphology. These materials are characterized by their strong photocapacitive response, which can be further enhanced by surface treatment with noble metals. Immersing the structures in solutions of $AgNO_3$, $HAuCl_4$, or K_2PtCl_4 in 1% HF produces junctions with concentrated metal centers decorating the surface. The presence of these metal centers dramatically increases the photocapacitive response, with 1 mM $HAuCl_4$ treatment leading to an approximately 11-fold increase in capacitive response and 325-fold increase in faradaic response, relative to the untreated structures. For the purposes of biological stimulation, however, even non-surface treated p-i-n junctions are sufficient for eliciting Ca^{2+} signals. Specifically, DRG cultures have been cultured on the surface, with optical stimulation achieved by selective illumination on a scanning confocal microscope. Cells show a large increase in cytosolic Ca^{2+} concentration upon illumination, a response that could be repeated several times without apparent damage to the cells.

In the same article, the authors used $HAuCl_4$-treated diode junctions embedded in PDMS, similar in concept to the meshes containing embedded NWs, to achieve organ-level stimulation. This includes traces from stimulated brain slices, as well as brains in vivo. For these experiments, they used the mesh-embedded junctions. While the total lifetime of in vivo applicability was not established, the devices were still competent of photonic stimulation after 14 days of degradation in phosphate-buffered saline solution. The in vivo experiments recorded increased neural activity readouts from channels that corresponded to the sensorimotor cortex. These responses spread to deeper layers over time, and their frequency scales with the power used for stimulation. Considering this ability to activate the sensorimotor cortex, they applied the mesh to either the left or right side of the forelimb primary motor cortex, and illuminated it. They found that this induced an up-and-down motion of the contralateral forelimb, consistent with expectations (Figure 5E,F). This shows the capability of the mesh system for exerting control over organisms' brains.

3.5. Upconversion Nanoparticles for Optical Modulation

As their name implies, upconversion nanoparticles (UCNPs) facilitate the conversion of multiple low-energy photons into a single high-energy photon.[81] This is typically achieved with heavy doping of trivalent lanthanides,[81,102] particularly thulium (Tm^{3+}) and ytterbium (Yb^{3+}). They are at their most biologically useful when the absorbance and emission

wavelengths both correspond to regions of the electromagnetic spectrum with desirable properties.

For example, recent work used UCNPs to facilitate two methods—photothermal and photodynamic—of cancer therapy.[103] This was possible because an upconverting shell could be formed around a polydopamine core without losing the photothermal character of the latter. In this case, the NPs absorbed in the near-infrared (NIR) range and emitted in the visible range, at far red and green wavelengths. NIR light was selected in this and other works using UCNPs for its particular ability to penetrate through tissue without encountering excessive scattering. The UCNPs were administered along with chlorin e6, a photosensitizer, and stimulated with NIR light, such that the emitted visible light interacted with the photosensitizer to produce singlet oxygen, while at the same time, the photothermal response locally heated the tissue.

A dramatic recent example entails using UCNPs to effectively enable near-infrared vision in mice.[46] The basic means by which this worked were as follows: the UCNPs were excited at NIR wavelengths (peak ≈ 950 nm) and emit in the visible realm at around 535 nm, which is the wavelength that humans perceive most efficiently.[104] The authors injected functionalized UCNPs into the sub-retinal spaces of mice and observed that the UCNPs were bound to rods and cones, with no apparent degradation after two months. They then tested the response of individual rods and found that the response from UCNP-injected mice at 950 nm was similar to the response at 535 nm. They further validated these results with behavioral studies of mice, finding that they responded to 950 nm light in ways that the control group did not (Figure 6A).

The principle of using UCNPs to specify light delivery is also exemplified by recent work combining UCNPs with optogenetic methods.[78] This helped to address an obstacle for optogenetic methods for neural and deep tissue stimulation: That low-power light does not penetrate to the needed tissue depths to actuate an optical response outside of the NIR region, but at the same time, commonly used optogenetic constructs cannot be engineered to respond to NIR light. By adding UCNPs to the technique, the problem is elegantly circumvented (Figure 6B). NIR light can be used to stimulate the UCNPs, which subsequently emit in the visible range, at wavelengths compatible with current limitations on the stimulation range for channel-rhodopsin-expressing neurons.[105]

3.6. Modulation of Nonexcitable Cells

A great deal of work has focused on modulating excitable cell types, due in large part to the simplicity of connecting electrical signaling to biological function in those cases. There is evidence to suggest that nonexcitable cells may be accessed without signaling through excitable cell types, however. There are in fact a number of studies that use mimics of endogenous electric fields to impact ostensibly nonexcitable cells, including modifying wound healing (Figure 6C)[75] and traction stress alignment[106] in epithelial tissues, as well as directional migration[107] and angiogenesis[76] in vascular endothelia. The mechanisms of stimulation are frequently more complicated than simply operating voltage-gated ion channels,[75,76] and in some instances it is unclear if voltage-gated Ca^{2+} channels, in particular, play a role[107–109] or are even present in the cells.[110]

Irrespective of whether they have been used for stimulation or not, many of the interfaces already mentioned have been found to be compatible with various types of nonexcitable cells. Silicon nanowires of various morphologies are internalized by human umbilical vein endothelial cells.[40,111] Likewise, porous silicon structures interface with the same cells and have been employed to modulate Ca^{2+} signaling through photothermal stimulation.[59]

3.7. Interface Formation as a Route to Modulation

Finally, recent work raises the exciting possibility of using interfaces themselves as paths to inducing biological change. It is well established that surface roughness in titanium implants can have an impact on the strength of the immune response to implantation.[58] With respect to nanoscale interfaces with tissues, surface topography has also been found to have physiological ramifications on the level of cells. One report, for instance, has identified topographically induced membrane curvature as a strong promoter of clathrin-mediated endocytosis.[64] Another study has identified a pathway through which membrane curvature can enhance polymerization of the cytoskeletal protein actin, and form branched structures around topographical features (Figure 6D).[65] Similar cytoskeletal rearrangements are actuated when the membrane is pierced by features with higher topographic prominence, that is, nanoneedles (Figure 2A).[112] In that case, actin has also been observed to accumulate around the nanoneedles, an effect that is accompanied by decreased nuclear expression of the mechanotransducer YAP,[112] which is indicative of a lower tendency for cells to spread out and to proliferate.[113] Taken together, these suggest a new way of looking at cell-material interfaces, one in which effects resulting from mechanical interactions are not necessarily side effects, but could also be engineered as part of a rational design to achieve a specific purpose.

4. Sensing

Sensing electrical currents in cells has been a major component of physiological studies since the earliest applications of micropipette electrode-based methods in the 1940s.[6] Later refinements of this method have introduced methods for intracellular and extracellular recording with ever-improving levels of detail,[114] as well as novel materials.[115] Within this framework, nanoscale FETs (nanoFETs) have emerged as useful tools for recording, as they are useful at length scales below what is achievable with micropipettes and microelectrodes,[116] and can be easily organized into arrays for multiplexed sensing.[79]

4.1. NanoFET Biosensors

Initial advances in applying nanoFETs to electrophysiological recording used kinks in silicon nanowires (SiNWs), together with modulating the doping profile during synthesis, to engineer source and drain arms separated by a short (≈200 nm) FET region near the vertex of the kinks.[116] The use of a sacrificial layer of poly (methylmethacrylate) with SU-8 flexible supports during synthesis yielded a device with a probe tip that extended out-of-plane and could be inserted for several seconds into cardiomyocytes to record electrical pulses during beating.[116]

A subsequent development in nanoFETs came with the introduction of branched nanowire FETs.[79] Briefly described, these devices consist of a region of p-type SiNW connected to source and drain terminals. A germanium nanowire branch is grown perpendicular to the axis of the NW and subsequently etched away after SiO_2 passivation, yielding a hollow tube of SiO_2 (Figure 7A). The small size of the tube allows it to penetrate into cells with minimal invasiveness. The device is capable of making sensitive electrical recordings, and due to its modularity, can be easily extended to an array format for making multiple simultaneous recordings over the course of 1 h.

4.2. 3D Self-Rolled Biosensor Arrays

As discussed in Interfaces, 3D self-rolled biosensor arrays (3D-SR-BAs) consist of an array of graphene FETs dispersed among metallic interconnects.[62] The mechanical design of the interconnects yields a structure that rolls itself into a hollow tube, which has been used to wrap around cardiac spheroids (Figure 7B, top) and deliver simultaneous recordings of the field potential at multiple sites around the encapsulated perimeter of the spheroid.

A key advantage offered by this device is the ability to take multiplexed recordings in three dimensions with high time resolution, with total recording durations up to three hours. This is in contrast to monitoring through confocal microscopy, in which each image captures only a single *xy*-plane, so that capturing the state of a whole organoid requires more time, on the order of minutes, than much of the signaling to be studied, on the order of seconds. Furthermore, the sensitivity of these recordings is enough to distinguish each individual ionic current across cell membranes within each beating cycle. Because the location of each FET or microelectrode sensor is known prior to the experiment, a 3D map of electric signal propagation can be assembled from the multiplexed recording. The progress of each current can also be measured at each given point in time to yield an accurate isochronal map[117] and the conduction speed in a given direction can be found by calculating the gradient of the isochronal map along that direction. Interestingly, the measured velocities on the order of 10 cm s^{-1}[62] agree with measurements taken from cardiomyocyte monolayers that are derived from human embryonic stem cells.[118]

4.3. Flexible Nanoelectronic Devices for Cyborg Organoids

Recordings from organoids interfaced with 3D sensor arrays, termed “cyborg organoids,” present another new development for bio-integrated electrical sensing.[61] The electronic component of cyborg organoids is formed from a 2D lattice arrangement of microelectrodes with serpentine interconnects that render the overall material very compliant, particularly when compared to the forces generated during subsequent integration with cells (Interfaces). While the initial structure is 2D, cells can be cultured on the device and subsequently induced to undergo organogenesis, yielding 3D organoids. Moreover, because the device is minimally invasive, it does not appear to induce excessive damage to the organoids, even over several weeks. During the development process, the electrode mesh remains associated with the organoid, adopting whatever conformation develops. Recordings from each electrode therefore monitor the local field potential at regularly spaced intervals around the organoid surface (Figure 7C).

Since the microelectrodes are located at regular intervals, the multiplex signals can be combined to form a 3D map of electrical signal propagation through organoids. As such, the development of electrical signaling regulation can be monitored over the entire course of organogenesis (Figure 7D). As might be expected, the electrophysiology of an organoid varies considerably over the process of development. Most notably, the dynamics of depolarization and repolarization becomes more pronounced at later times. That is, the fast part of depolarization increases significantly in amplitude, while the duration of the depolarizing current increases only slightly during the same time.

5. Conclusion

We have presented here only a small subset of the many recent and current developments taking place in nano-bioelectronics. In particular, a wide variety of methods for eliciting biological responses are under development, whether those arise from mechanical interactions with implanted devices or from electrophysiological stimulation. As our understanding of the space of these interactions deepens, we should be able to elucidate the electrical, mechanical, and biochemical pathways that are involved in each case. Furthermore, refined techniques for modulation and sensing, as well as delivery systems, should enable integrated devices that can detect and correct pathological states, with or without external control.

Acknowledgements

E.N.S. would like to thank Kelliann Koehler and Theresa Chmiel for copyediting assistance and helpful feedback, as well as Margaret L. Gardel for invaluable scientific support and guidance.

Biographies

Erik Schaumann received his B.S. in chemistry from Santa Clara University in 2013, where he performed research with Dr. Amelia A. Fuller on self-associating water soluble peptoids (N-substituted glycine oligomers). He began his Ph.D. studies at the University of Chicago in 2014, where he has worked under the advisement of Dr. Margaret L. Gardel and Dr. Bozhi Tian. His research interests span the intersection of mechanobiology, nanotechnology, and bioelectronics.

Bozhi Tian received the B.S. and M.S. degrees in chemistry from Fudan University Shanghai, China, and the A.M. and Ph.D. degrees in physical chemistry from Harvard University in 2010. As an associate professor in the Department of Chemistry at the University of Chicago, his current research focuses on the semiconductor-enabled understanding of subcellular biophysics, as well as studies of dynamics at soft-hard interfaces.

References

[1]. Walsh J, Philos. Trans 1773, 63, 461.

[2]. Faraday M, Philos. Trans 1839, 129, 1.

[3]. Ling G, Gerard RW, J. Cell. Comp. Physiol 1949, 34, 383. [PubMed: 15410483]

[4]. Marmont G, J. Cell. Comp. Physiol 1949, 34, 351. [PubMed: 15406358]

[5]. Hodgkin AL, Huxley AF, Proc. R. Soc. B 1952, 140, 177. [PubMed: 13003922]

[6]. Schwiening CJ, J. Physiol 2012, 590, 2571. [PubMed: 22787170]

[7]. Bhandari R, Negi S, Solzbacher F, Biomed. Microdevices 2010, 12, 797. [PubMed: 20480240]

[8]. Jun JJ, Steinmetz NA, Siegle JH, Denman DJ, Bauza M, Barbarits B, Lee AK, Anastassiou CA, Andrei A, Aydin C, Barbic M, Blanche TJ, Bonin V, Couto J, Dutta B, Gratiy SL, Gutnisky DA, Hausser M, Karsh B, Ledochowitsch P, Lopez CM, Mitelut C, Musa S, Okun M, Pachitariu M, Putzeys J, Rich PD, Rossant C, Sun WL, Svoboda K, Carandini M, Harris KD, Koch C, O'Keefe J, Harris TD, Nature 2017, 551, 232. [PubMed: 29120427]

[9]. Steinmetz NA, Koch C, Harris KD, Carandini M, Curr. Opin. Neurobiol 2018, 50, 92. [PubMed: 29444488]

[10]. Ganzer PD, Sharma G, Neural Regener. Res 2019, 14, 46.

[11]. George JA, Kluger DT, Davis TS, Wendelken SM, Okorokova EV, He Q, Duncan CC, Hutchinson DT, Thumser ZC, Beckler DT, Marasco PD, Bensmaia SJ, Clark GA, Sci. Rob 2019, 4, eaax2352.

[12]. Mickle AD, Won SM, Noh KN, Yoon J, Meacham KW, Xue Y, Mcllvried LA, Copits BA, Samineni VK, Crawford KE, Kim DH, Srivastava P, Kim BH, Min S, Shiuan Y, Yun Y, Payne MA, Zhang J, Jang H, Li Y, Lai HH, Huang Y, Il Park S, Gereau RW, Rogers JA, Nature 2019, 565, 361. [PubMed: 30602791]

[13]. Jin Y, Gao X, Nat. Nanotechnol 2009, 4, 571. [PubMed: 19734929]

[14]. Tian B, Zheng X, Kempa TJ, Fang Y, Yu N, Yu G, Huang J, Lieber CM, Nature 2007, 449, 885. [PubMed: 17943126]

[15]. Zhu Y, Murali S, Cai W, Li X, Suk JW, Potts JR, Ruoff RS, Adv. Mater 2010, 22, 3906. [PubMed: 20706983]

[16]. Jansen R, Nat. Mater 2012, 11, 400. [PubMed: 22522640]

[17]. Sinova J, Valenzuela SO, Wunderlich J, Back CH, Jungwirth T, Rev. Mod. Phys 2015, 87, 1213.

[18]. Acarón Ledesma H, Li X, Carvalho-de-Souza JL, Wei W, Bezanilla F, Tian B, Nat. Nanotechnol 2019, 14, 645. [PubMed: 31270446]

[19]. Zhang A, Lieber CM, Chem. Rev 2016, 116, 215. [PubMed: 26691648]

[20]. Zhou W, Dai X, Lieber CM, Rep. Prog. Phys 2017, 80, 016701. [PubMed: 27823988]

[21]. Sakhrani NM, Padh H, Drug Des. Devel. Ther 2013, 7.

[22]. Haziza S, Mohan N, Loe-Mie Y, Lepagnol-Bestel AM, Massou S, Adam MP, Le XL, Viard J, Plancon C, Daudin R, Koebel P, Dorard E, Rose C, Hsieh FJ, Wu CC, Potier B, Herault Y, Sala C, Corvin A, Allinquant B, Chang HC, Treussart F, Simonneau M, Nat. Nanotechnol 2017, 12, 322. [PubMed: 27893730]

[23]. Chipaux M, van der Laan KJ, Hemelaar SR, Hasani M, Zheng T, Schirhagl R, Small 2018, 14, 1704263.

[24]. Mohan N, Chen CS, Hsieh HH, Wu YC, Chang HC, Nano Lett 2010, 10, 3692. [PubMed: 20677785]

[25]. Ho D, Wang CHK, Chow EKH, Sci. Adv 2015, 1, e1500439. [PubMed: 26601235]

[26]. Moore L, Yang J, Lan TTH, Osawa E, Lee DK, Johnson WD, Xi J, Chow EKH, Ho D, ACS Nano 2016, 10, 7385. [PubMed: 27439019]

[27]. Fakhri N, Wessel AD, Willms C, Pasquali M, Klopfenstein DR, MacKintosh FC, Schmidt CF, Science 2014, 344, 1031. [PubMed: 24876498]

[28]. Kumar S, Rani R, Dilbaghi N, Tankeshwar K, Kim KH, Chem. Soc. Rev 2017, 46, 158. [PubMed: 27841412]

[29]. Heister E, Brunner EW, Dieckmann GR, Jurewicz I, Dalton AB, ACS Appl. Mater. Interfaces 2013, 5, 1870. [PubMed: 23427832]

[30]. Cheng C, Li S, Thomas A, Kotov NA, Haag R, Chem. Rev 2017, 117, 1826. [PubMed: 28075573]

[31]. Tu Z, Guday G, Adeli M, Haag R, Adv. Mater 2018, 30, 1.

[32]. Zeglio E, Rutz AL, Winkler TE, Malliaras GG, Herland A, Adv. Mater 2019, 31, 1806712.

[33]. Shi Z, Phillips GO, Yang G, Nanoscale 2013, 5, 3194. [PubMed: 23512106]

[34]. Wang Z, Tammela P, Stromme M, Nyholm L, Adv. Energy Mater 2017, 7, 1.

[35]. Duan X, Huang Y, Cui Y, Wang J, Lieber CM, Nature 2001, 409, 66. [PubMed: 11343112]

[36]. Luo Z, Jiang Y, Myers BD, Isheim D, Wu J, Zimmerman JF, Wang Z, Li Q, Wang Y, Chen X, Dravid VP, Seldman DN, Tian B, Science 2015, 348, 1451. [PubMed: 26113718]

[37]. Yang C, Zhong Z, Lieber CM, Science 2005, 310, 1304. [PubMed: 16311329]

[38]. Gupta AK, Gupta M, Biomaterials 2005, 26, 3995. [PubMed: 15626447]

[39]. Kabashin AV, Evans P, Pastkovsky S, Hendren W, Wurtz GA, Atkinson R, Pollard R, Podolskiy VA, Zayats AV, Nat. Mater 2009, 8, 867. [PubMed: 19820701]

[40]. Zimmerman JF, Parameswaran R, Murray G, Wang Y, Burke M, Tian B, Sci. Adv 2016, 2, e1601039. [PubMed: 28028534]

[41]. Chiappini C, Martinez JO, De Rosa E, Almeida CS, Tasciotti E, Stevens MM, ACS Nano 2015, 9, 5500. [PubMed: 25858596]

[42]. Reina G, González-Domínguez JM, Criado A, Vázquez E, Bianco A, Prato M, Chem. Soc. Rev 2017, 46, 4400. [PubMed: 28722038]

[43]. Feig VR, Tran H, Bao Z, ACS Cent. Sci 2018, 4, 337. [PubMed: 29632879]

[44]. Parameswaran R, Carvalho-De-Souza JL, Jiang Y, Burke MJ, Zimmerman JF, Koehler K, Phillips AW, Yi J, Adams EJ, Bezanilla F, Tian B, Nat. Nanotechnol 2018, 13, 260. [PubMed: 29459654]

[45]. Chiappini C, De Rosa E, Martinez JO, Liu X, Steele J, Stevens MM, Tasciotti E, Nat. Mater 2015, 14, 532. [PubMed: 25822693]

[46]. Ma Y, Bao J, Zhang Y, Li Z, Zhou X, Wan C, Huang L, Zhao Y, Han G, Xue T, Cell 2019, 177, 243. [PubMed: 30827682]

[47]. Liu J, Fu TM, Cheng Z, Hong G, Zhou T, Jin L, Duvvuri M, Jiang Z, Kruskal P, Xie C, Suo Z, Fang Y, Lieber CM, Nat. Nanotechnol 2015, 10, 629. [PubMed: 26053995]

[48]. Tseng Y, Kole TP, Wirtz D, Biophys. J 2002, 83, 3162. [PubMed: 12496086]

[49]. Celis JE, Biochem. J 1984, 223, 281. [PubMed: 6093771]

[50]. Gopal S, Chiappini C, Penders J, Leonardo V, Seong H, Rothery S, Korchev Y, Shevchuk A, Stevens MM, Adv. Mater 2019, 31, 1806788.

[51]. Xu AM, Kim SA, Wang DS, Aalipour A, Melosh NA, Lab Chip 2016, 16, 2434. [PubMed: 27292263]

[52]. Xu AM, Wang DS, Shieh P, Cao Y, Melosh NA, ChemBioChem 2017, 18, 623. [PubMed: 28130882]

[53]. Cao Y, Hjort M, Chen H, Birey F, Leal-Ortiz SA, Han CM, Santiago JG, Pasca SP, Wu JC, Melosh NA, Proc. Natl. Acad. Sci. U. S. A 2017, 114, E1866. [PubMed: 28223521]

[54]. Rotenberg MY, Yamamoto N, Schaumann EN, Matino L, Santoro F, Tian B, Proc. Natl. Acad. Sci. U. S. A 2019, 116, 22531. [PubMed: 31624124]

[55]. Dante S, Petrelli A, Petrini EM, Marotta R, Maccione A, Alabastri A, Quarta A, De Donato F, Ravasenga T, Sathya A, Cingolani R, Proietti Zaccaria R, Berdondini L, Barberis A, Pellegrino T, ACS Nano 2017, 11, 6630. [PubMed: 28595006]

[56]. Walters R, Kraig RP, Medintz I, Delehanty JB, Stewart MH, Susumu K, Huston AL, Dawson PE, Dawson G, ASN Neuro 2012, 4, AN20120042.

[57]. Walters R, Medintz IL, Delehanty JB, Stewart MH, Susumu K, Huston AL, Dawson PE, Dawson G, ASN Neuro 2015, 7, 175909141559238.

[58]. Agarwal R, Domowicz MS, Schwartz NB, Henry J, Medintz I, Delehanty JB, Stewart MH, Susumu K, Huston AL, Deschamps JR, Dawson PE, Palomo V, Dawson G, ACS Chem. Neurosci 2015, 6, 494. [PubMed: 25688887]

[59]. Jiang Y, Carvalho-De-Souza JL, Wong RCS, Luo Z, Isheim D, Zuo X, Nicholls AW, Jung IW, Yue J, Liu DJ, Wang Y, De Andrade V, Xiao X, Navrazhnykh L, Weiss DE, Wu X, Seidman DN, Bezanilla F, Tian B, Nat. Mater 2016, 15, 1023. [PubMed: 27348576]

[60]. Jiang Y, Li X, Liu B, Yi J, Fang Y, Shi F, Gao X, Sudzilovsky E, Parameswaran R, Koehler K, Nair V, Yue J, Guo KH, Fang Y, Tsai HM, Freyermuth G, Wong RCSS, Kao CM, Chen CT, Nicholls AW, Wu X, Shepherd GMGG, Tian B, Nat. Biomed. Eng 2018, 2, 508. [PubMed: 30906646]

[61]. Li Q, Nan K, Le Floch P, Lin Z, Sheng H, Blum TS, Liu J, Nano Lett 2019, 19, 5781. [PubMed: 31347851]

[62]. Kalmykov A, Huang C, Bliley J, Shiwarski D, Tashman J, Abdullah A, Rastogi SK, Shukla S, Mataev E, Feinberg AW, Jimmy Hsia K, Cohen-Karni T, Sci. Adv 2019, 5, eaax0729. [PubMed: 31467978]

[63]. Parameswaran R, Koehler K, Rotenberg MY, Burke MJ, Kim J, Jeong KY, Hissa B, Paul MD, Moreno K, Sarma N, Hayes T, Sudzilovsky E, Park HG, Tian B, Proc. Natl. Acad. Sci. U. S. A 2019, 116, 413. [PubMed: 30538202]

[64]. Zhao W, Hanson L, Lou HY, Akamatsu M, Chowdary PD, Santoro F, Marks JR, Grassart A, Drubin DG, Cui Y, Cui B, Nat. Nanotechnol 2017, 12, 750. [PubMed: 28581510]

[65]. Lou HY, Zhao W, Li X, Duan L, Powers A, Akamatsu M, Santoro F, McGuire AF, Cui Y, Drubin DG, Cui B, Proc. Natl. Acad. Sci. U. S. A 2019, 116, 23143. [PubMed: 31591250]

[66]. Discher DE, Janmey P, Wang Y, Science 2005, 310, 1139. [PubMed: 16293750]

[67]. Oakes PW, Banerjee S, Marchetti MC, Gardel ML, Biophys. J 2014, 107, 825. [PubMed: 25140417]

[68]. Engler AJ, Sen S, Sweeney HL, Discher DE, Cell 2006, 126, 677. [PubMed: 16923388]

[69]. Weisenhorn AL, Khorsandi M, Kasas S, Gotzos V, Butt H-J, Nanotechnology 1993, 4, 106.

[70]. Wegst UGK, Bai H, Saiz E, Tomsia AP, Ritchie RO, Nat. Mater 2015, 14, 23. [PubMed: 25344782]

[71]. Elliott H, Fischer RS, Myers KA, Desai RA, Gao L, Chen CS, Adelstein RS, Waterman CM, Danuser G, Nat. Cell Biol 2015, 17, 137. [PubMed: 25621949]

[72]. Irons HR, Cullen DK, Shapiro NP, Lambert NA, Lee RH, LaPlaca MC, J. Neural Eng 2008, 5, 333. [PubMed: 18756031]

[73]. Aradhya SV, Frei M, Hybertsen MS, Venkataraman L, Nat. Mater 2012, 11, 872. [PubMed: 22886066]

[74]. Feiner R, Wertheim L, Gazit D, Kalish O, Mishal G, Shapira A, Dvir T, Small 2019, 15, 1805526.

[75]. Zhao M, Song B, Pu J, Wada T, Reid B, Tai G, Wang F, Guo A, Walczysko P, Gu Y, Sasaki T, Suzuki A, Forrester JV, Bourne HR, Devreotes PN, McCaig CD, Penninger JM, Nature 2006, 442, 457. [PubMed: 16871217]

[76]. Zhao M, Bai H, Wang E, Forrester JV, McCaig CD, J. Cell Sci 2004, 117, 397. [PubMed: 14679307]

[77]. Chen Y, Ye L, Guan L, Fan P, Liu R, Liu H, Chen J, Zhu Y, Wei X, Liu Y, Bai H, Biol. Open 2018, 7, bio035204. [PubMed: 30232195]

[78]. Chen S, Weitemier AZ, Zeng X, He L, Wang X, Tao Y, Huang AJY, Hashimotodani Y, Kano M, Iwasaki H, Parajuli LK, Okabe S, Loong Teh DB, All AH, Tsutsui-kimura I, Tanaka KF, Liu X, Mchugh TJ, Science 2018, 359, 679. [PubMed: 29439241]

[79]. Duan X, Gao R, Xie P, Cohen-Karni T, Qing Q, Choe HS, Tian B, Jiang X, Lieber CM, Nat. Nanotechnol 2012, 7, 174.

[80]. Fang Y, Jiang Y, Ledesma HA, Yi J, Gao X, Weiss DE, Shi F, Tian B, Acaron Ledesma H, Yi J, Gao X, Weiss DE, Shi F, Tian B, Nano Lett 2018, 18, 4487. [PubMed: 29894630]

[81]. Suyver JF, Aebischer A, Biner D, Gerner P, Grimm J, Heer S, Krämer KW, Reinhard C, Güdel HU, Optical Materials 2005, 27, 1111.

[82]. Jiang Y, Tian B, Nat. Rev. Mater 2018, 3, 473. [PubMed: 31656635]

[83]. Pankove JI, Optical Processes in Semiconductors, Dover Publications, Inc., New York 1975.

[84]. Shu Y, Fales BS, Peng W, Levine BG, J. Phys. Chem. Lett 2017, 8, 4091. [PubMed: 28799771]

[85]. Holm AN, Rich A, Sarr MG, Farrugia G, Am. J. Physiol.-Gastrointest. Liver Physiol 2000, 279, G1155. [PubMed: 11093937]

[86]. Nerbonne JM, Kass RS, Physiol. Rev 2005, 85, 1205. [PubMed: 16183911]

[87]. Edd JF, Horowitz L, Rubinsky B, IEEE Trans. Biomed. Eng 2005, 52, 695. [PubMed: 15825871]

[88]. Shapiro MG, Homma K, Villarreal S, Richter CP, Bezanilla F, Nat. Commun 2012, 3, 10.1038/ncomms1742.

[89]. Kawai K, Larson BJ, Ishise H, Carre AL, Nishimoto S, Longaker M, Lorenz HP, PLoS One 2011, 6, e27106. [PubMed: 22073267]

[90]. Ringer S, J. Physiol 1883, 4, 29.

[91]. Miller DJ, J. Physiol 2004, 555, 585. [PubMed: 14742734]

[92]. Tian W, Hou C, Ren Z, Wang C, Zhao F, Dahlbeck D, Hu S, Zhang L, Niu Q, Li L, Staskawicz BJ, Luan S, Nature 2019, 572, 131. [PubMed: 31316205]

[93]. Clapham DE, Cell 2007, 131, 1047. [PubMed: 18083096]

[94]. Abzhanov A, Kuo WP, Hartmann C, Grant BR, Grant PR, Tabin CJ, Nature 2006, 442, 563. [PubMed: 16885984]

[95]. Mallarino R, Grant PR, Grant BR, Herrel A, Kuo WP, Abzhanov A, Proc. Natl. Acad. Sci. U. S. A 2011, 108, 4057. [PubMed: 21368127]

[96]. Zhang CH, Wang P, Liu DH, Chen CP, Zhao W, Chen X, Chen C, He WQ, Qiao YN, Tao T, Sun J, Peng YJ, Lu P, Zheng K, Craige SM, Lifshitz LM, Keaney JF, Fogarty KE, Ge RZ, Zhu MS, Nat. Commun 2016, 7, 1.

[97]. Wang Q, Chen M, Schafer NP, Bueno C, Song SS, Hudmon A, Wolynes PG, Neal Waxham M, Cheung MS, Proc. Natl. Acad. Sci. U. S. A 2019, 116, 18937. [PubMed: 31455737]

[98]. Allen GM, Mogilner A, Theriot JA, Curr. Biol 2013, 23, 560. [PubMed: 23541731]

[99]. Fang Y, Jiang Y, Ledesma HA, Yi J, Gao X, Weiss DE, Shi F, Tian B, Nano Lett 2018, 18, 4487. [PubMed: 29894630]

[100]. Nattel S, Cardiovasc. Res 2018, 114, 349. [PubMed: 29360945]

[101]. Quinn TA, Camelliti P, Rog-Zielinska EA, Siedlecka U, Poggioli T, O'Toole ET, Knopfel T, Kohl P, Proc. Natl. Acad. Sci. U. S. A 2016, 113, 14852. [PubMed: 27930302]

[102]. Liu Y, Lu Y, Yang X, Zheng X, Wen S, Wang F, Vidal X, Zhao J, Liu D, Zhou Z, Ma C, Zhou J, Piper JA, Xi P, Jin D, Nature 2017, 543, 229. [PubMed: 28225761]

[103]. Yan S, Zeng X, Tang Y, Liu BF, Wang Y, Liu X, Adv. Mater 2019, 31, 1.

[104]. Bieber ML, Volbrecht VJ, Werner JS, Vision Res 1995, 35, 1385. [PubMed: 7645267]

[105]. Nagel G, Szellas T, Huhn W, Kateriya S, Adeishvili N, Berthold P, Ollig D, Hegemann P, Bamberg E, Proc. Natl. Acad. Sci. U. S. A 2003, 100, 13940. [PubMed: 14615590]

[106]. Cho Y, Son M, Jeong H, Shin JH, Mol. Biol. Cell 2018, 29, 2292. [PubMed: 30044714]

[107]. Kim JM, Lee M, Kim N, Do Heo W, Proc. Natl. Acad. Sci. U. S. A 2016, 113, 5952. [PubMed: 27190091]

[108]. Luckhoff A, Busse R, Arch. Pharmacol 1990, 94.

[109]. Andrikopoulos P, Fraser SP, Patterson L, Ahmad Z, Burcu H, Ottaviani D, Diss JKJ, Box C, Eccles SA, Djamgoz MBA, J. Biol. Chem 2011, 44, 1.

[110]. Vargas FF, Caviedes PF, Grant DS, Microvasc. Res 1994, 47, 153. [PubMed: 7517490]

[111]. Zimmerman JF, Murray GF, Wang Y, Jumper JM, Austin JR, Tian B, Nano Lett 2015, 15, 5492. [PubMed: 26192816]

[112]. Hansel CS, Crowder SW, Cooper S, Gopal S, Da Cruz M. Joaio Pardelha, De Oliveira Martins L, Keller D, Rothery S, Becce M, Cass AEG, Bakal C, Chiappini C, Stevens MM, ACS Nano 2019, 13, 2913. [PubMed: 30829469]

[113]. Aragona M, Panciera T, Manfrin A, Giulitti S, Michielin F, Elvassore N, Dupont S, Piccolo S, Cell 2013, 154, 1047. [PubMed: 23954413]

[114]. Chorev E, Epsztein J, Houweling AR, Lee AK, Brecht M, Curr. Opin. Neurobiol 2009, 19, 513. [PubMed: 19735997]

[115]. Hai A, Shappir J, Spira ME, Nat. Methods 2010, 7, 200. [PubMed: 20118930]

[116]. Tian B, Cohen-Karni T, Qing Q, Duan X, Xie P, Lieber CM, Science 2010, 329, 830. [PubMed: 20705858]

[117]. Ideker RE, Smith WM, Blanchard SM, Reiser SL, Simpson EV, Wolf PD, Danieley ND, Pacing Clinical Electrophysiol 1989, 12, 456.

[118]. Thompson SA, Burridge PW, Lipke EA, Shamblott Mi, Zambidis ET, Tung L, J. Mol. Cell. Cardiol 2012, 53, 15. [PubMed: 22713758]

[119]. Schaumann EN, Tian B, Proc. Natl. Acad. Sci. U. S. A 2019, 116, 22897. [PubMed: 31645378]

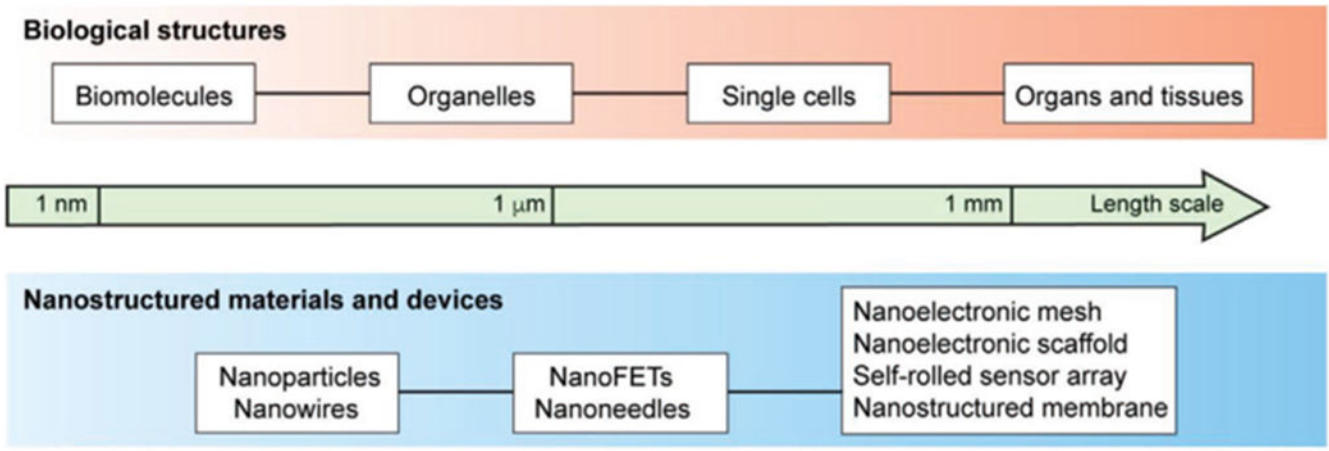

Figure 1.

Schematic illustration of the subjects in this Progress Report. Top: Biological targets for interactions with nano-bioelectronics can be as small as individual molecules and can interface up to the level of entire organs and tissues. Bottom: Selected nanostructured materials and devices discussed in this article.

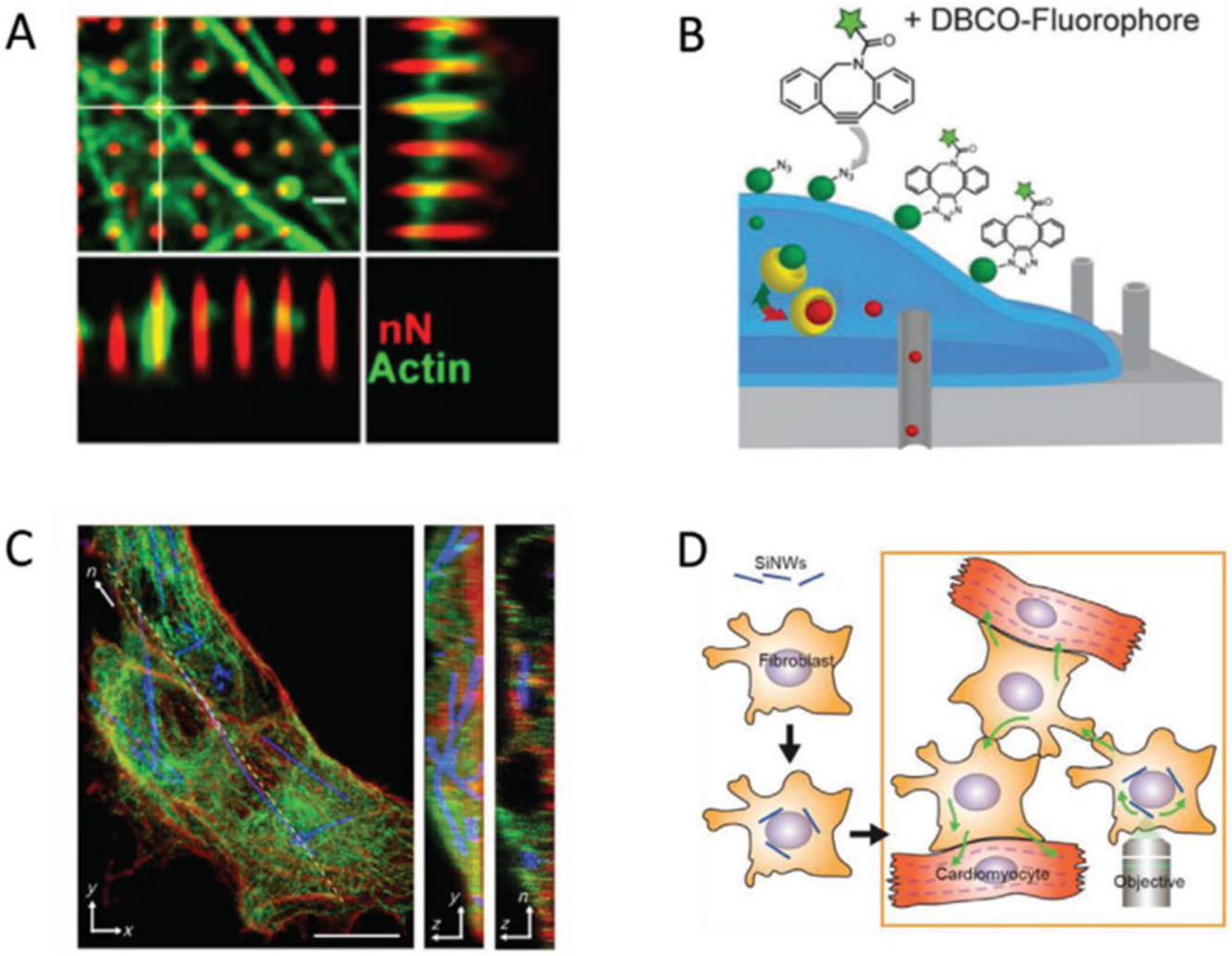

Figure 2.

Selected examples of intracellular nano-biointerfaces. A) Human mesenchymal stem cells grown on porous silicon nanoneedles. The cytoskeletal protein actin (green) can accumulate around nanoneedles (red). Scale bar = 10 μm. Adapted with permission.[112] Copyright 2019, American Chemical Society. B) Diagram of nanostraws being used to deliver markers of protein glycosylation. The nanostraws (gray cylinders) can access the intracellular space, so that an azidosugar cargo (red spheres) can enter the cell. In the instance pictured, the azidosugar is subsequently converted to sialic acid groups (green spheres) and transported to the cell surface, where they can be fluorescently labeled. Adapted with permission.[52] Copyright 2017, John Wiley and Sons. C) Silicon nanowires spontaneously internalized by human umbilical vein endothelial cells. Actin (red) and tubulin (green) indicate the cytoskeletal architecture of the cell, showing that nanowires (blue) incorporate well with the cytoskeleton. Scale bar = 10 μm. Reproduced with permission.[40] Copyright 2016, American Association for the Advancement of Science (AAAS). D) Diagram of how hybridized cells can be employed to access cells that do not normally internalize nanowires. In this instance, cardiomyocytes do not internalize the cells, but they can interface with

cardiac myofibroblasts, which do. The myofibroblast-nanowire hybrids can then be stimulated such that the resultant effects are transmitted to the myocytes. Adapted with permission.[54] Copyright 2019, National Academy of Sciences.

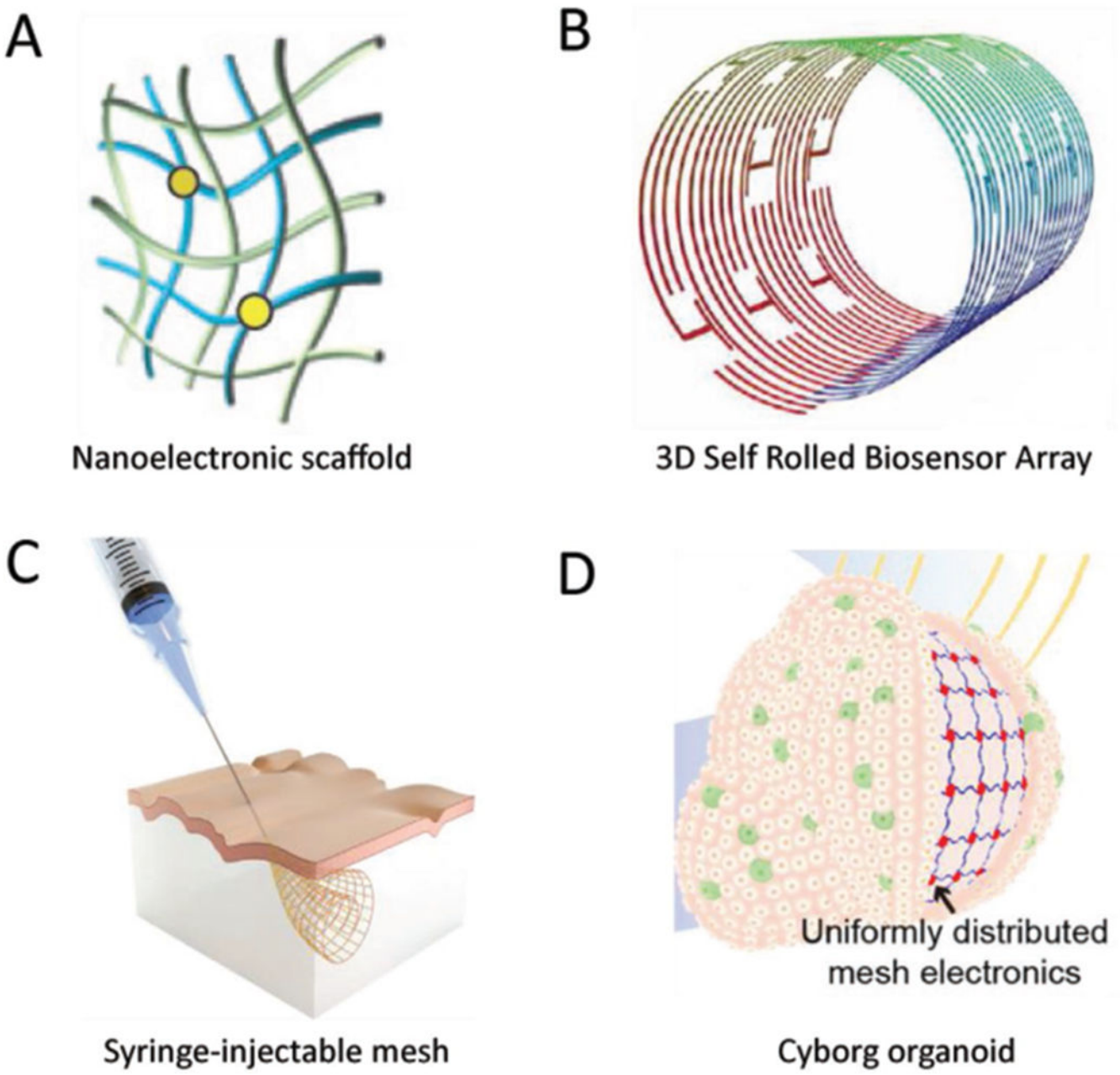

Figure 3.

Developments regarding bioelectronic interfaces for cells and tissues in three dimensions. A) Nanoelectronic scaffolds consist of silicon-based FETs interconnected by a polymer/metal-coated polymer mesh. The mesh structure can be tuned to either fold itself into a given shape, or to else be amenable to subsequent manipulation to form rolled or folded structures. Adapted with permission.[73] Copyright 2012, Springer Nature. B) Diagram of a 3D self-rolled biosensor array (3D-SR-BA). The structures are engineered with residual stresses along the interconnects, such that after liftoff the device rolls itself into a cylindrical sensor. The radius of curvature can be controlled by the amount of residual stress, making the arrays amenable to interfacing with cardiac spheroids of different sizes. Adapted with permission.

[62] Copyright 2019, AAAS. C) Design principle for syringe injectable electronics. Serpentine interconnects in a rhomboidal lattice motif are exceptionally flexible in the transverse direction, but stiff in the longitudinal direction. They can therefore roll up tightly to pass through fine gauges of needles without buckling, and subsequently expand after delivery. Adapted with permission.[47] Copyright 2015, Springer Nature. D) Flexible nanoelectronic arrays for integration with organoids. Serpentine interconnects with an initial planar structure form tight interfaces with 2D developing organs. As the cells undergo organogenesis and the concomitant 2D to 3D transition, the array alters its conformation to match the organoid. The resulting cyborg organoid allows for electrical monitoring across the entire surface of the 3D structure. Adapted with permission.[61] Copyright 2019, American Chemical Society.

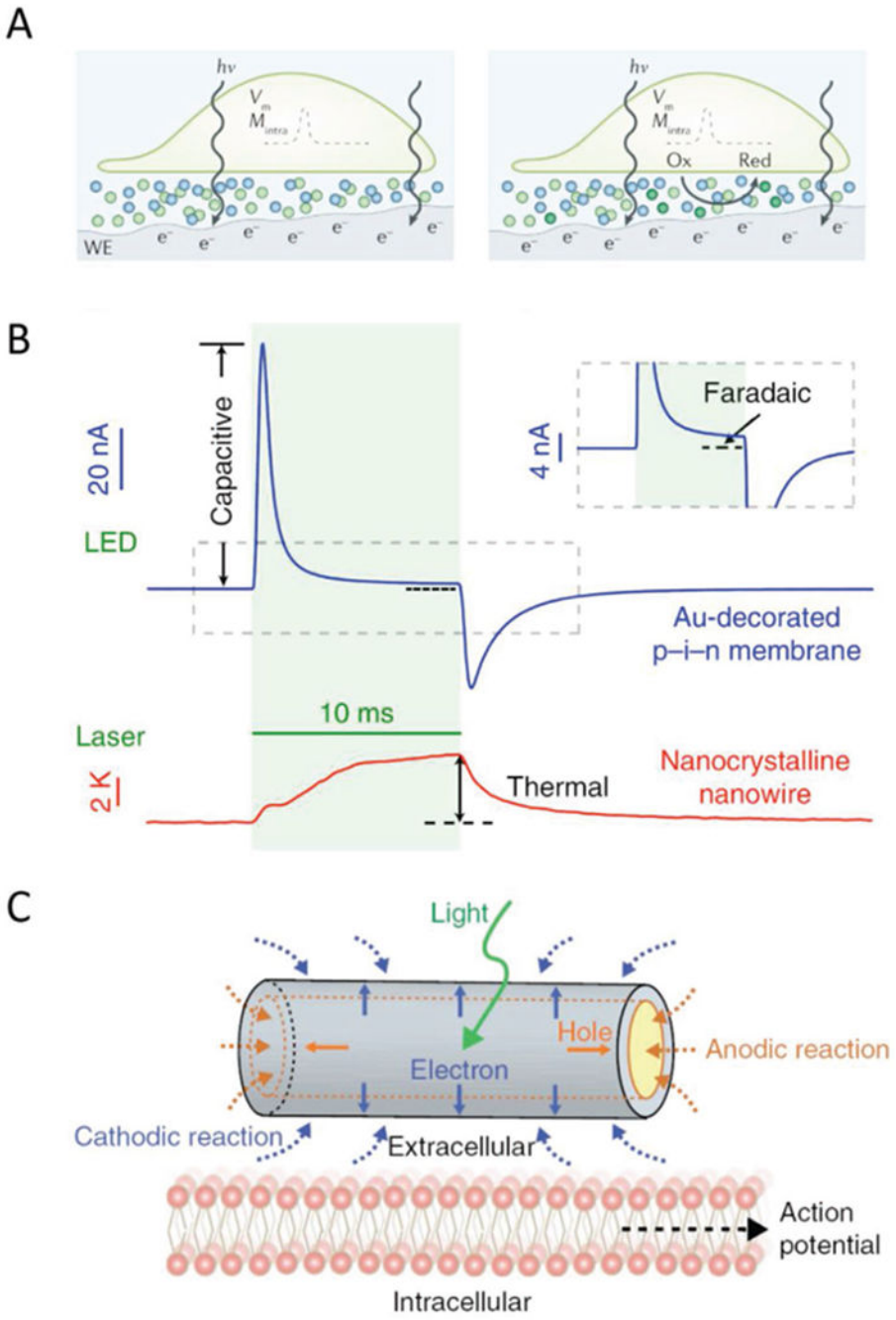

Figure 4.

Mechanisms of photoresponses for semiconductor-based nano-bioelectronic devices. A) Illustrations of the photocapacitive (left) and photofaradaic (right) response from the semiconductor working electrode, labeled WE, in biological settings. Electrode-electrolyte interfaces form electrical double layers. The capacitive response occurs when photostimulation induces a capacitive discharge of the double layer, producing a relatively large, transient current. The photofaradaic response comes from the steady rate of charge transfer due to redox reactions taking place with accumulated charge carriers from

illumination. Adapted with permission.[82] Copyright 2018, Springer Nature. B) Traces of photocapactive, photofaradaic, and photothermal responses in planar diode junctions and silicon nanowires, respectively. The photothermal response is a consequence of nonradiative recombination in the depletion zone. Adapted with permission.[60] Copyright 2018, Springer Nature. C) Schematic of the photofaradaic response with coaxial p-i-n SiNWs. Electrons on the n-type shall facilitate reduction reactions around the NW surface, while holes that accumulate in the p-type zone can only participate in oxidation reactions on the exposed shell regions on the NW ends. Adapted with permission.[44] Copyright 2018, Springer Nature.

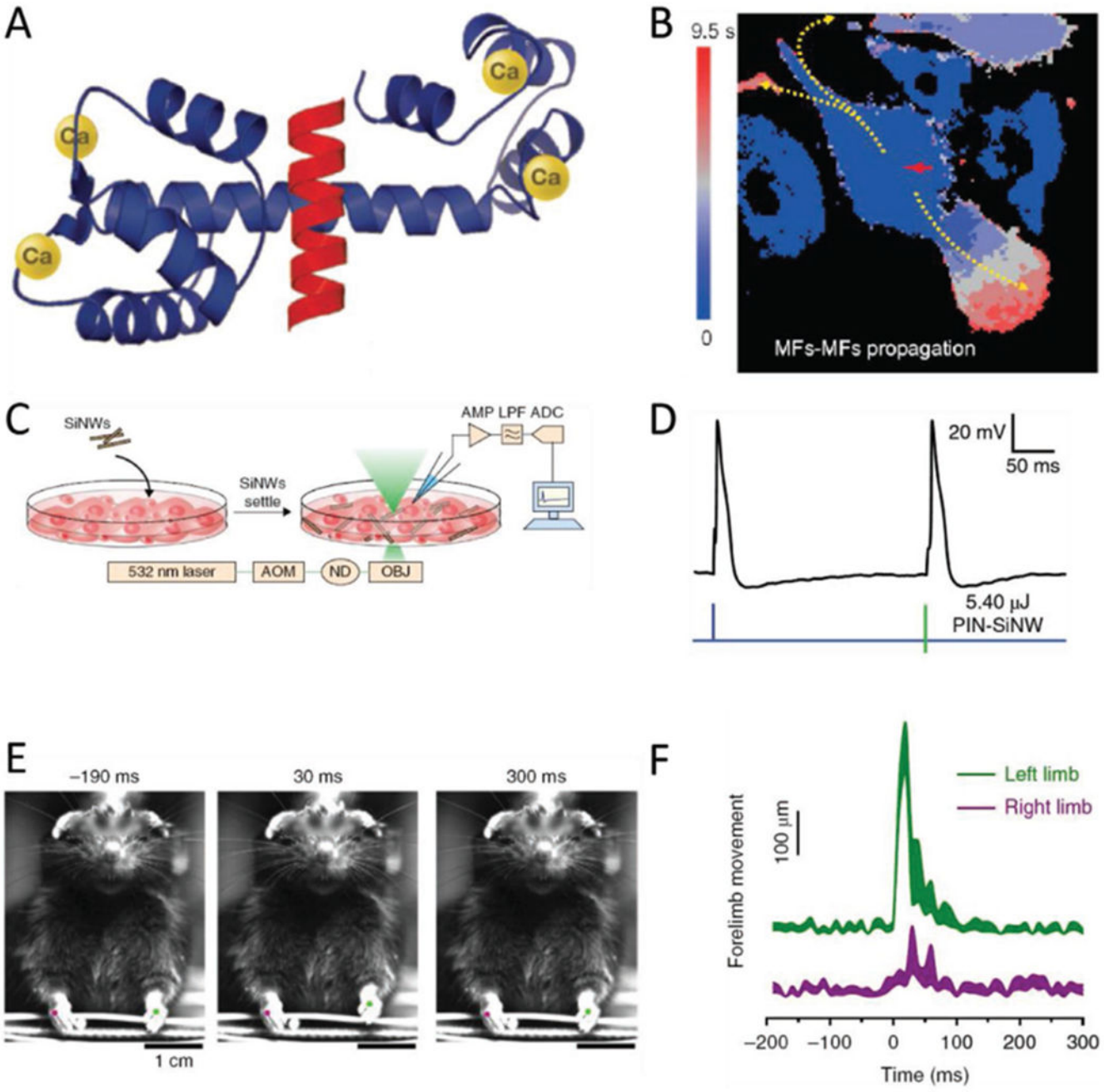

Figure 5.

Biological modulation with Si-based nanostructured materials. A) Structure of the protein calmodulin, which chelates four Ca^{2+} ions and in response exposes binding sites that interface with other proteins. Calcium signals are transduced to a vast array of biological responses through the action of CaM. Adapted with permission.[93] Copyright 2007, Cell Press. B) Selective illumination of SiNW-bearing myofibroblasts cocultured with cardiomyocytes yields calcium fluxes that transmit to adjacent cells through different mechanisms based on cell type. MF to CM communication takes place faster than the time resolution of the imaging, while MF to MF signal transmission is considerably slower.

Adapted with permission.[54] Copyright 2019, National Academy of Sciences. C) Illustration of the experimental setup used in stimulating dorsal root ganglion cultures. SiNWs are added to cultured cells and given time to interact with the cells. The system is imaged and stimulated on a confocal microscope, with recording of the membrane potential achieved via a patch clamp apparatus. Adapted with permission.[44] Copyright 2018, Springer Nature. D) Dorsal root ganglion neurons interfaced with SiNWs show a calcium response to illumination, which occurs alongside action potential elicitation. The photonically induced AP (right hand spike in the trace) is comparable to an AP induced from direct current injection (left hand spike). Adapted with permission.[44] Copyright 2018, Springer Nature. E) Planar diode junctions embedded in PDMS mesh enable light-based control of rat forelimb motion. The PDMS conforms to the shape of rat brains, so that multiple areas in the sensorimotor cortex to be stimulated. When the mesh is placed on one hemisphere of the brain, illumination results in the contralateral forelimb being noticeably raised. Adapted with permission.[60] Copyright 2018, Springer Nature. F) Trace of the forelimbs from the rat pictured in panel E, showing that photostimulation induces the left forelimb to be raised. Adapted with permission.[60] Copyright 2018, Springer Nature.

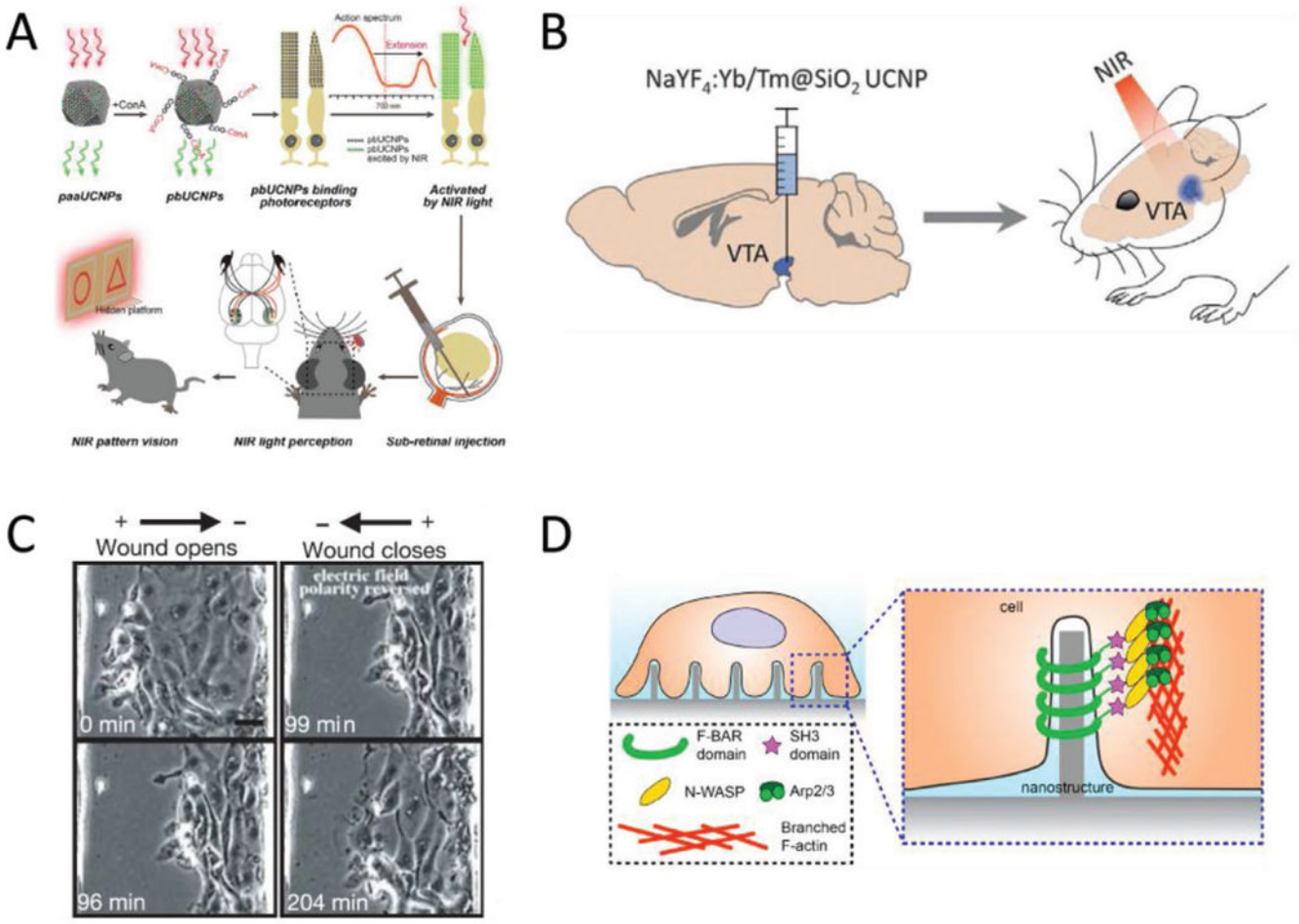

Figure 6.

Other biointerface devices for enacting systemic changes. A) Schematic of the UCNP-based method for enabling NIR vision in rats. The UCNPs absorb at 950 nm and emit at 535 nm. Injections of surface modified UCNPs to the sub-retinal space eventually produces "nanoantannae," hybrids of the UCNPs and rod optical sensors. Subsequent training and experiments indicated the injected rats could discern NIR light, while control groups could not. Reproduced with permission.[46] 2019, Cell Press. B) Optogenetic techniques can be expanded to deep tissue stimulation by pairing optogenetic constructs with UCNPs. The ability of UCNPs to convert NIR light to the visible region resolves the incompatibility with the light scattering effect of tissues and the existing range of wavelengths that can actuate optogenetic proteins. Adding UCNPs to the protocol means that NIR light, which has the optimal tissue penetration, can be converted to blue light, which activates channelrhodopsin, deep in the brain. Adapted with permission.[78] Copyright 2018, AAAS. C) Electric fields at physiological magnitudes (150 mV mm^{-1}) impact the progress of wound healing in epithelial cells—an example of bioelectronics impacting non-excitable cell types. In this instance, the polarity of the externally applied field determined whether the opening would open or close over time. Scale bar = 20 μm. Reproduced with permission.[75] Copyright 2006, Springer Nature. D) Geometry as a possible avenue for device-based targeted modulation. Nanoscale surface features can trigger the cytoskeletal protein actin to

accumulate at regions of curvature when the radius is under the 400 nm threshold. The curvature-dependent actin accumulation is indicative of the possibility for devices that take advantage of both electrical and morphological cues, provided respectively by the device functionality and the geometry of the implant. Reproduced with permission.[119] Copyright 2019, National Academy of Sciences.

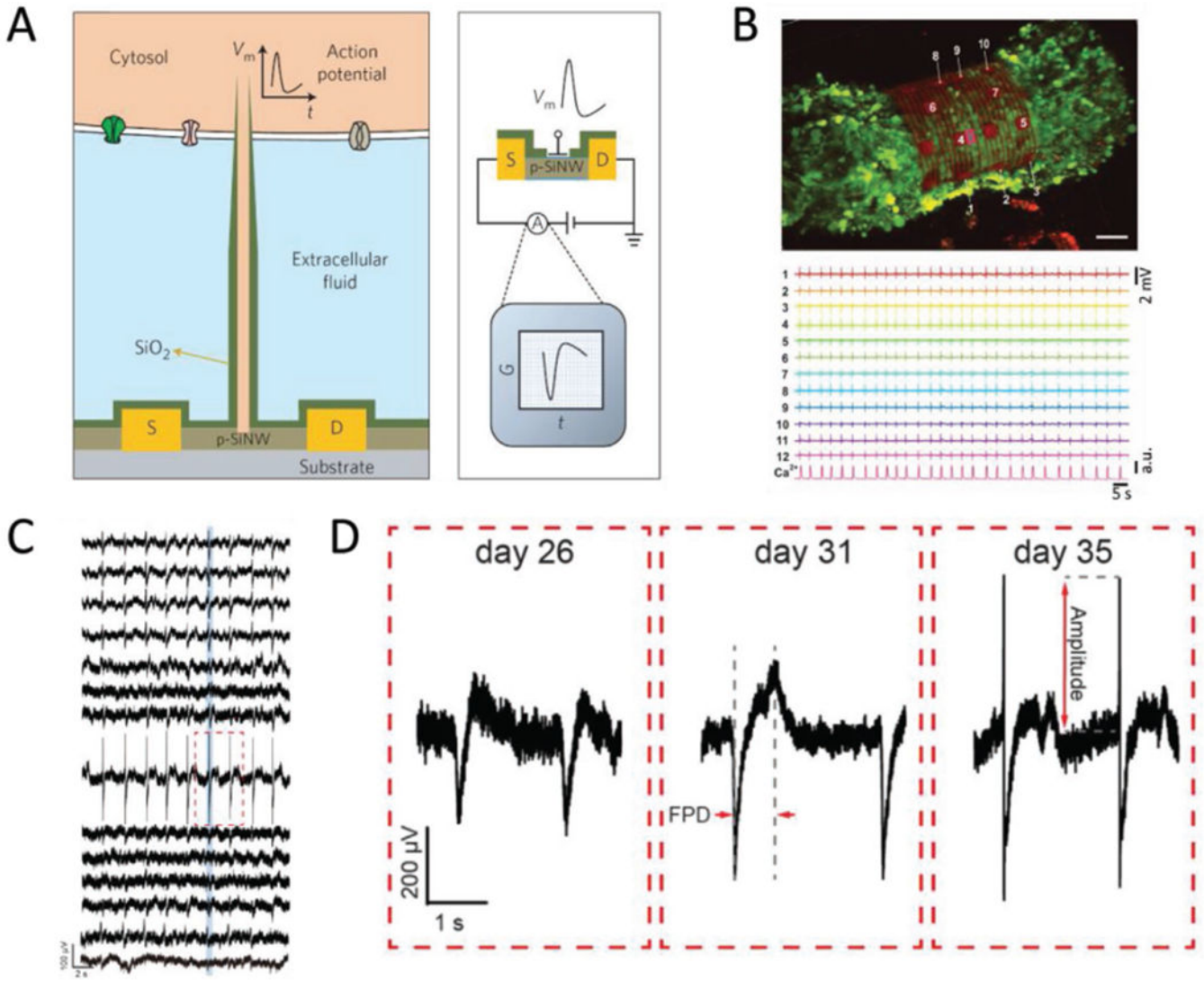

Figure 7.

A survey of nanoelectronic biosensors. A) Schematic of a branched nanowire FET sensor for intracellular recording. A p-type SiNW spine connects to source and drain terminals, with tube-shaped protrusions used to access the intracellular space. A layer of SiO_2 passivates the device and insulates the tube from the extracellular fluid. Reproduced with permission.[79] Copyright 2012, Springer Nature. B) 3D self rolled biosensor array enclosing a cardiac spheroid. Sensors placed around the 3D-SR-BA (numbered white arrows, top image) enable high resolution simultaneous recording (bottom traces) of electrical signals throughout the 3D structure, which cannot currently be achieved using confocal microscopy. Scale bar = 50 μm. Reproduced with permission.[62] Copyright 2019, AAAS. C) Traces of the multiplexed recording from the cyborg organoid on day 35. The sensors were distributed throughout the device mesh, such that each trace represents a different sampling region that together cover the entire organoid surface. Adapted with permission.[61] Copyright 2019, American Chemical Society. D) Close up of the red boxed region in panel (C), taken at different stages of organoid development. As organogenesis proceeds, the amplitude of the spike gets bigger,

which tracks the regulation of electrical signaling during the organ's development. Adapted with permission.[61] Copyright 2019, American Chemical Society.